

Journal of Biomedical Optics

SPIEDigitalLibrary.org/jbo

***Ex vivo* determination of glucose permeability and optical attenuation coefficient in normal and adenomatous human colon tissues using spectral domain optical coherence tomography**

Qingliang Zhao
Chuanqing Zhou
Huajiang Wei
Yonghong He
Xinyu Chai
Qiushi Ren

Ex vivo determination of glucose permeability and optical attenuation coefficient in normal and adenomatous human colon tissues using spectral domain optical coherence tomography

Qingliang Zhao,^a Chuanqing Zhou,^a Huajiang Wei,^b Yonghong He,^c Xinyu Chai,^a and Qiushi Ren^d

^aShanghai Jiao Tong University, School of Biomedical Engineering, No. 800 Dongchuan Road, Shanghai 200240, China

^bSouth China Normal University, MOE Key Laboratory of Laser Life Science and Institute of Laser Life Science, Guangzhou 510631, Guangdong Province, China

^cTsinghua University, Laboratory of Optical Imaging and Sensing, Graduate School at Shenzhen, Shenzhen 518055, China

^dPeking University, College of Engineering, Department of Biomedical Engineering, Beijing 100871, China

Abstract. Recent reports have suggested that spectral domain optical coherence tomography (SD-OCT) is a useful tool for quantifying the permeability of hyperosmotic agents in various tissues. We report our preliminary results on quantification of glucose diffusion and assessment of the optical attenuation change due to the diffusion of glucose in normal and adenomatous human colon tissues *in vitro* by using a SD-OCT and then calculated the permeability coefficients (PC) and optical attenuation coefficients (AC). The PC of a 30% aqueous solution of glucose was $3.37 \pm 0.23 \times 10^{-6}$ cm/s in normal tissue and $5.65 \pm 0.16 \times 10^{-6}$ cm/s in cancerous colon tissue. Optical AC in a normal colon ranged from 3.48 ± 0.37 to 2.68 ± 0.82 mm⁻¹ and was significantly lower than those seen in the cancerous tissue (8.48 ± 0.95 to 3.16 ± 0.69 mm⁻¹, $p < 0.05$). The results suggest that quantitative measurements of using PC and AC from OCT images could be a potentially powerful method for colon cancer detection. © 2012 Society of Photo-Optical Instrumentation Engineers (SPIE). [DOI: 10.1117/1.JBO.17.10.105004]

Keywords: permeability coefficient; glucose; attenuation coefficient; colon adenocarcinoma; spectral domain optical coherence tomography.

Paper 12208 received Mar. 31, 2012; revised manuscript received Aug. 31, 2012; accepted for publication Sep. 5, 2012; published online Oct. 1, 2012.

1 Introduction

It was estimated that more than one million new cases of colorectal cancer were clinically diagnosed in 2008. This disease kills nearly half a million people worldwide each year, with the majority of these patients suffering from adenocarcinomas.¹ Early stages of colon adenocarcinoma can change the macro-architecture of the colon tissue, and mainly include an increase in microvascularisation, the blood content of the tissue lesion,² and the distortion of collagen matrix.³ In addition, the significant increase in the concentration of blood and proteins in the cancerous tissue over that in normal tissue may lead to the differences in optical properties and permeability of an analyte between normal and malignant human colon tissues. In other words, the abnormalities in malignant tissues can alter physical and physiological properties of the specimen and can cause the change of diffusion rate of a certain analyte.⁴ Measurement and understanding of these changes could be utilized to detect and identify the cancerous tissue, which may be helpful for the early diagnosis of colon cancer.

Currently, colonoscopy is the most commonly technique used for early detection of colorectal cancer, but this method is only capable of surface visualization, which limits its ability

to detect precancerous changes.⁵ Endoscopic ultrasound, which is capable of depth-resolved imaging, is currently used in the clinical and research settings, but its resolution in standard devices is limited.⁶ Hence, early detection of neoplastic changes before metastasis remains a critical objective in colorectal cancer diagnosis and treatment. Modern optics can provide real-time imaging of human tissues with resolutions that are comparable to that of histopathology, as well as having the potential ability to reveal biochemical and/or molecular information. These modern optical approaches could significantly improve the identification of malignancies at curable stages.⁷

Optical coherence tomography (OCT), a noninvasive technology for microstructure imaging of biological tissues, has been used to quantify the permeability of a hyperosmotic agent in atherosclerotic vascular tissue, cancerous gastric tissue, breast cancer tissue, and sclera and skin tissues *ex vivo* and *in vivo*.⁸⁻¹² Additionally, OCT can be used for localized quantitative measurement of attenuation coefficients (AC), which can provide additional information for discrimination of the different tissues.¹³⁻¹⁵ The scattering properties of the tissue depend on the difference of refractive index-matching between the cells and extracellular fluid.¹⁶ Partially applying an analyte can reduce the optical discontinuity in the extracellular fluid and the cell membrane, and therefore, reduce light scattering. OCT has been used to discriminate different structural features of the normal and atherosclerotic vascular tissues,¹⁷ apoptosis and necrosis in

Address all correspondence to: Chuanqing Zhou, School of Biomedical Engineering, Shanghai Jiao Tong University, No. 800 Dongchuan Road, Shanghai 200240, China. Tel: +86-21-34204076; Fax: +86-21-34204078; E-mail: zhucq@sjtu.edu.cn; Qiushi Ren, Peking University, College of Engineering, Department of Biomedical Engineering, Beijing 100871, China. Tel: +86-10-62767113; Fax: +86-10-62767113; E-mail: renqsh@coe.pku.edu.cn

human fibroblasts. This shows that OCT is sensitive to the changes of the attenuation coefficient caused by analyte diffusion, which is induced by morphological changes of biological tissue.¹⁸ Thus, we can adopt the OCT technique for assessing the differences of permeability coefficients (PC) and AC in normal and cancerous tissues caused by hyperosmotic agents. This could assist in distinguishing cancerous from nonmalignant tissue, and possibly result in early colon diagnosis.

In this paper we report the results of our studies on the real-time monitoring, differentiation, and quantification of diffusion of the glucose solution in human normal and adenomatous colon tissues *in vitro* using spectral domain OCT (SD-OCT). Finally, we also compare the characteristics of the glucose permeability and optical AC properties of normal and malignant colon tissue. The results show PC and AC calculated from OCT images are helpful for the detection of cancerous colon tissue in the early stages.

2 Materials and Methods

2.1 SD-OCT System

Ex vivo experiments were performed with a custom-built SD-OCT system, the schematic of which is shown in Fig. 1. A broadband super luminescent diode light source (SLD, Inphenix Co. Ltd., Livermore, CA) was used as the optical source. The central wavelength, bandwidth, and output power were 830 nm, 40 nm and 5 mW, respectively, with the light source coupled into a 50/50 optical fiber coupler. Then the interference signal of the light beam reflected from the reference and sample arms was collected by using a spectrometer, which consisted of a transmitting grating (1200-line/mm), focus lens ($f = 200$ mm), and a linear CCD camera (2048 pixels, $14 \mu\text{m}/\text{pixel}$, e2V). The system operated at an A-scan frequency of 20 kHz, the signal-to-noise ratio was measured at 120 dB and the frame rate was 20 fps. The axial and transverse resolution was 12 and $15 \mu\text{m}$, respectively. Two-dimensional (2-D) images were obtained by scanning the incident beam over the sample surface in the lateral direction. The SD-OCT system operation was entirely controlled by a personal computer. Two-dimensional OCT images were acquired from each experiment and stored for post-processing.

2.2 Materials and Measurements

Patients volunteered for the research program conducted at the Second Affiliated Clinical Hospital of Guangzhou University of

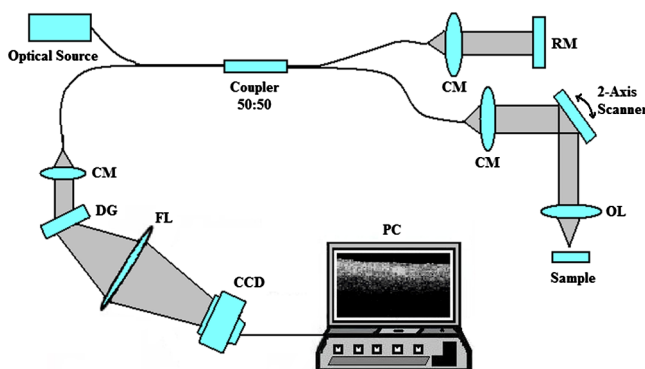


Fig. 1 Schematic drawing of the SD-OCT system: (CM-collimator, DG-diffraction grating, FL-focusing lens, RM-reference mirror and OL-objective lens) used in the experiment.

Traditional Chinese Medicine, China and signed consent forms, with the procedure being approved by the local Ethics Committee. Colon tissue samples were stored in 0.9% sodium chloride solution after the resection, and then placed on ice and transported to the laboratory for performing measurements as soon as possible. All the samples were divided into two groups according to pathological diagnosis: normal colon tissues (11 samples), adenomatous colon tissues (11 samples). In order to ensure the hydration and colon tissue samples integrity, each sample was rinsed briefly in saline to remove excess surface blood and fat tissue. Each colon sample tissue was stored in a refrigerator at -70°C , and then was cut into approximately 1.5×1.5 cm size pieces for *in vitro* measurement. As in previous studies,¹⁹⁻²¹ to guarantee the minimal changes in the physiological status and optical properties of low temperature samples, all tissue samples were prepared and measured within 12 h after removal. Prior to OCT imaging, tissue samples were brought to room temperature and defrosted in physiological saline for approximately 30 min. Baseline values were obtained from a selected region of the sample and monitored for approximately eight to 10 min prior to treatment with 30% glucose. The 30% glucose was then added to the colon tissues' sample surface for 5 min, then solutions carefully removed prior to OCT imaging. Every 30 min during the measurement, glucose was applied again on the tissue for 5 min. The 2-D images were continuously obtained by scanning the sample in the lateral and axial direction by the OCT. Each sample was used only once. The entire *ex vivo* OCT imaging was monitored for approximately 2 h at room temperature (22°C) throughout the experiment. A 30% glucose (Tianjin Damao Chemical Reagent Factory, China) solution in dH_2O , with the mean refractive index of 1.39,²² was used in the diffusion experiments. A reasonable assumption for the average refractive index of colon tissue is $n > 1.4$.²³

2.3 Calculation Methods

The PC of the glucose in the tissues were determined by analyzing the changes in the slope of OCT signal intensity induced by the glucose diffusion in a specific depth region. This method was described in detail in previously reported works.²⁴⁻²⁸ A one-dimensional (1-D) curve displaying the distribution of OCT signal intensity in depth plotted in a logarithmic scale was created by averaging the 2-D images laterally. A region in the 1-D OCT signal intensity profile was chosen where the signal was relatively linear and with minimal oscillations. The slope was then calculated from the chosen intensity profile for further analysis,^{29,30} with the calculated OCT signal slopes (OCTSS) normalized and plotted as a function of time. The PC of 30% glucose in the normal and malignant colon tissue was calculated using the following equation: ($\dot{P} = z_{\text{region}}/t_{\text{region}}$), where P is the permeability coefficient, z_{region} is the thickness of the chosen section, and t_{region} is the time for the glucose to diffuse through that section.^{8,11,31} The penetration time was measured from the point where the OCTSS started to decrease to the point at which the reverse process began.

The optical attenuation coefficient of the tissue can be quantified from the intensity of the detected light versus the depth. For media with absorption as described by the single-scattering approximation, the light travels in a ballistic way and Beer's law can be applied to calculate the total OCT attenuation coefficient: $\mu_t = \mu_a + \mu_s$, where μ_a is the absorption coefficient and μ_s is the scattering coefficient.³² These are physical properties unique to

the biological tissue, which play a vital role in the assessment of the tissue feature.^{15,33,34} In this current OCT system case, the measured signal is defined as:^{15,33–35}

$$[\langle i^2(z) \rangle]^{\frac{1}{2}} \approx (\langle i^2 \rangle_0)^{\frac{1}{2}} [\exp(-2\mu_t z)]^{\frac{1}{2}}, \quad (1)$$

where the $\langle i^2(z) \rangle$ is the photo detector heterodyne signal current received by an OCT system from the probing depth z and the mean square heterodyne signal $\langle i^2 \rangle_0$. The result of the OCT study is the measurement of optical backscattering or reflectance $R(z) \propto [\langle i^2(z) \rangle]^{1/2}$ from a tissue versus axial ranging distance, or depth, z . The reflectance depends on the optical properties of tissue, i.e., the total attenuation coefficient μ_t . Thus, combined with Eq. (1) and $R(z)$ it follows that the reflected power can be approximately proportional to $-\mu_t z$ in exponential scale according to the single scattering model:

$$R(z) = I_0 a(z) \exp(-\mu_t z). \quad (2)$$

Here I_0 is the optical power launched into the tissue sample and $a(z)$ is the reflectivity of the tissue sample at the depth of z . Therefore, measurement of OCT reflectance for depths z_1 and z_2 allows for approximately evaluating the attenuation coefficient and its temporal behavior. This evaluation is due to reduction of the tissue-scattering coefficient at the agent immersion if reflectivity $a(z)$ is considered as weakly dependent on depth for a homogeneous tissue layer. The μ_t theoretically can be obtained from the reflectance intensity measurements at two different depths, z_1 and z_2 :^{15,33–35}

$$\mu_t = \frac{1}{\Delta z} \ln \left[\frac{R(z_1)}{R(z_2)} \right], \quad (3)$$

where $\Delta z = |z_1 - z_2|$. For more details about the entire formulas derivation process, check Ref. 36. Noise is inevitable in the measurement, thus a final result should be obtained using a least-square fitting method in order to improve the accuracy of determining μ_t value. An averaged intensity profile as a function of depth was obtained by averaging the 2-D images laterally

over approximately 1 mm, which was enough for speckle noise suppression. A best-fit exponential curve was applied to the averaged intensity profiles of each group since the noise in the measurement is unavoidable.

2.4 Statistical Analysis

The data from all samples were presented as means \pm SD and analyzed by an SPSS 16.0 software paired-test. The $p < 0.05$ value indicated significant difference.

3 Results and Discussion

Figure 2(a) to 2(c) showed OCT images of normal colon tissue 0, 15, and 30 min after the topical application of 30% glucose, and Fig. 2(d) to 2(f) showed images of the cancerous colon tissue. Normal colon tissue had a regular and compact appearance and layers were clearly visible, but the cancerous tissue structure appeared disorganized, nonuniform and had many dark crypts. Comparison of Fig. 2(a) and 2(d) demonstrated a remarkable difference between the normal and malignant colon tissue: the backscattering from the cancerous tissue appeared more heterogeneous than that of normal colon tissue. In addition, the cancerous tissue appeared to have a higher scattering than the normal colon tissue, which was most likely due to larger cell nuclei, higher nuclear-to-cytoplasmic ratio, and higher regional tumor cell density in tumor colon tissue.³⁷ Figure 2 also showed that the visibility, contrast, and imaging depth in both tissues were significantly improved after the application of glucose. This change resulted from the diffusion of the topically applied analyte into the extracellular and intracellular space. A refractive index matching environment was created by matching the chemical agents with the main scattering components within the tissue, leading to the enhanced light penetration. And the light penetration was further enhanced with the reduced light scattering due to the dehydration effect after the glucose application.^{38,39}

The typical dynamic change of the 1-D OCT normalized signal intensity profiles and corresponding exponential best-fit curves in the experiments were shown in Fig. 3. The degree

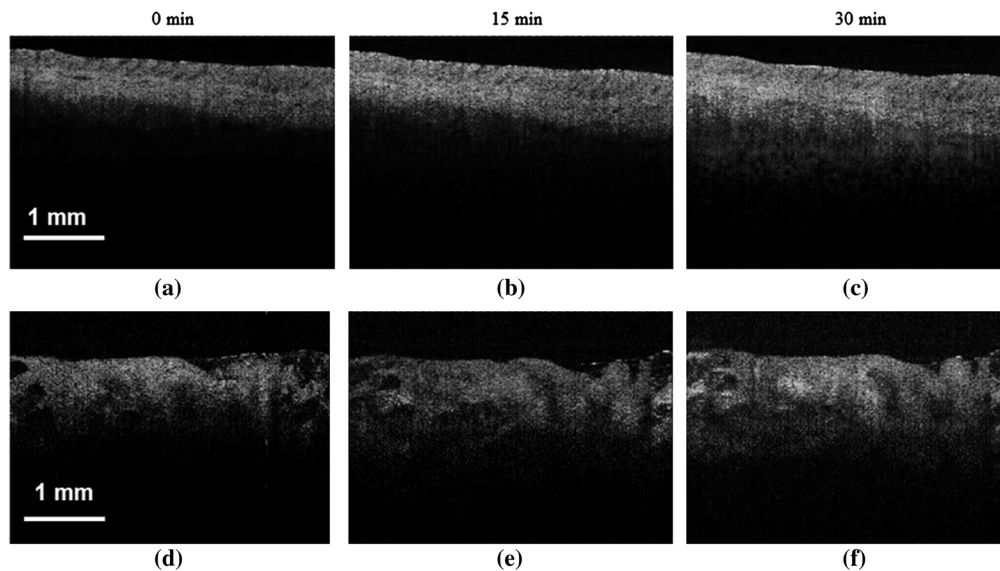


Fig. 2 OCT images of normal (a)–(c) and the adenomatous colon tissue (d)–(f) at 0, 15, and 30 min, (respectively) after the application of a 30% glucose solution.

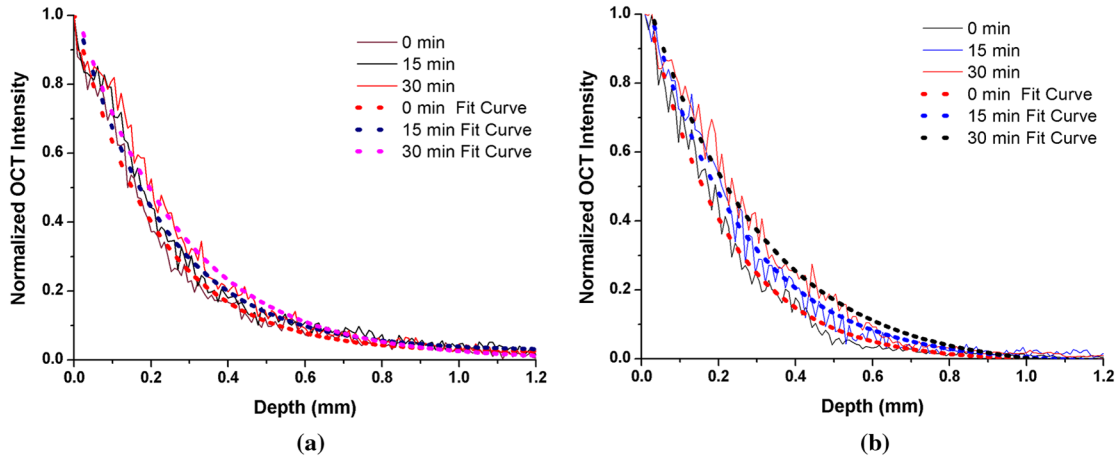


Fig. 3 Normalized OCT intensity profiles with their corresponding exponential best fit curves zero, 15 and 30 min after the topical application of 30% glucose; (a) normal colon tissue and (b) adenomatous colon tissue.

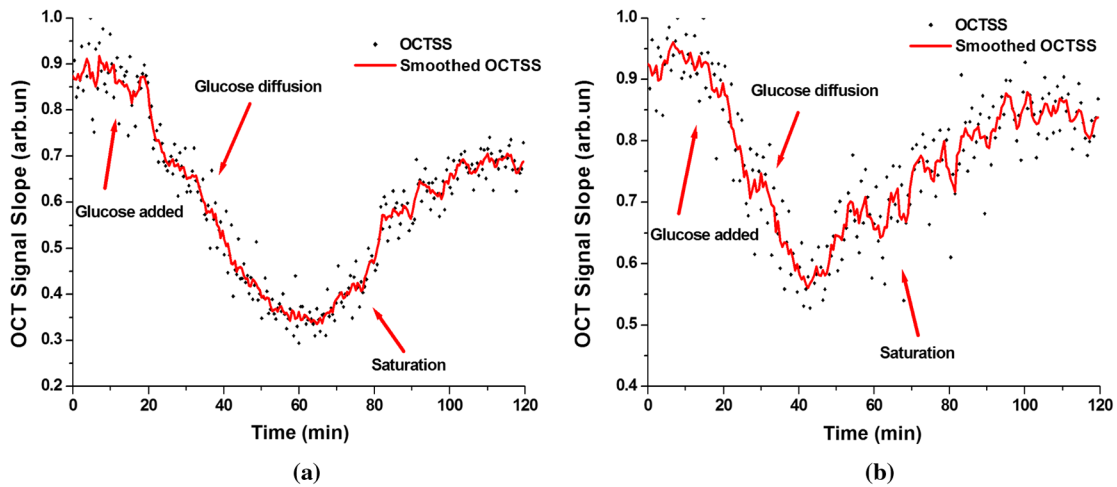


Fig. 4 The typical OCTSS graphs for human normal (a) and adenocarcinoma (b) colon tissues during a 30% glucose diffusion experiment, respectively.

of change in the OCT signal intensity increased coincided with the glucose penetration of internal structures and a concomitant increase in glucose concentration. The cancerous tissues yielded a much broader but steeper OCT signal profile from Fig. 3(b) than that observed in the normal colon tissue between zero to -30 min. These results may be due to the additive effect of the glucose diffusion, which enhances light transportation into the tissue. Thus more photons propagated to the deep reflective surfaces underneath the tissue give rise to a stronger back-reflected signal. OCTSS was calculated from an axial 95- μm region at a tissue depth of approximately 296 μm away from the tissue surface. As shown in Fig. 4, a similar trend was observed in the normal and malignant colon tissue. The dynamic OCTSS decreased due to a reduction of light scattering inside the tissue, which was caused by a local increase in glucose concentration with the increase in time. It is also apparent that the OCTSS decrease in cancerous tissue was faster than that of normal tissue, as shown in Fig. 4(a) and 4(b). In Fig. 4(a), glucose reached the monitored region approximately 20 min after application and took another 47 min for it to completely achieve the diffusion process. In contrast, for the cancer

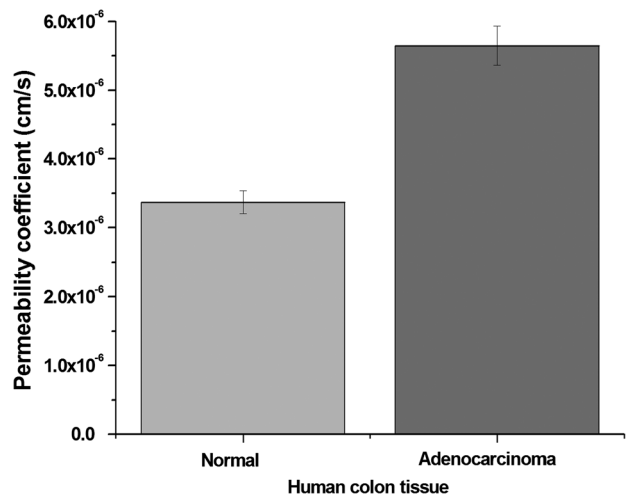


Fig. 5 Comparison of the mean permeability coefficient of 30% glucose diffusion in normal human and adenocarcinoma colon tissues.

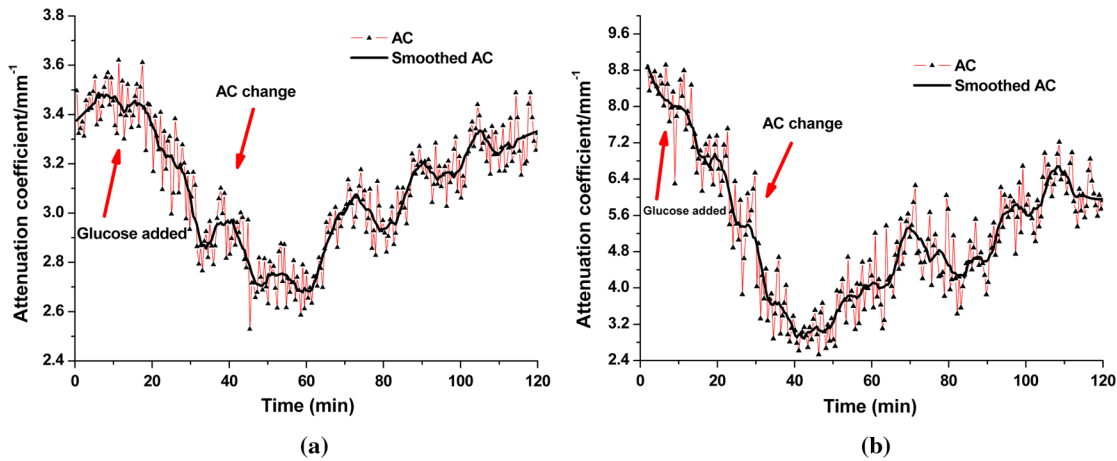


Fig. 6 Mean attenuation coefficients of normal (a) and adenomatous colon tissues (b) after topical application of 30% glucose.

tissue, it only took about 13 min to reach the monitored region, and then another 41 min to completely diffuse the whole region in Fig. 4(b). At that point, a reverse process in the OCTSS was observed. This reverse process could be due to diffusion via concentration gradient differences on either side of the tissue. The net fluid (mainly water) movement from high concentration areas to lower concentration will occur, such that induced water re-enters the tissue after diffusing out until equilibrium is reached.^{10,11,40} The PC of 30% glucose for the normal colon tissue in Fig. 5 was significantly slower at $3.37 \pm 0.17 \times 10^{-6}$ cm/s compared with the PC in the adenomatous colon tissue $5.65 \pm 0.24 \times 10^{-6}$ cm/s ($p < 0.05$).

Analysis of the decrease in the OCT signal allowed us to quantitatively determine the optical AC using the OCT technique.^{41,42} The mean OCT signal from a region of tissue was determined by the specific local optical properties of the region of interest. Quantification of these intrinsic optical properties can provide an extra objective, classification parameter.⁴² In both cases, the optical AC decreased with the length of time following topical application of the glucose. This may be due to the glucose diffusion into the tissue, wherein tissue contrast is caused mainly by the coefficients of tissue attenuation. And the coefficients of tissue attenuation depend on the tissue interstitial space volume fraction, cell diameters, and tissue architecture. The AC of normal tissue was found to differ significantly from other cancer components with the continuous diffusion of glucose into the tissues [Fig. 6(a) and 6(b)]. In our study the decrease of light attenuation was much more prominent in the cancer tissue than that of normal tissue in the same region where we determined the OCTSS. It also can be seen from Fig. 6(a) and 6(b) that the AC seemed to undertake periodic oscillations when the glucose was added to the tissues. This may be related to some exchange processes in the glucose and differently-sized and -hydrated (collagen, elastin) structures of tissue because of glucose osmotic impact inducing water flux from (dehydration) these structures and back (rehydration) to them inside tissue.⁴³ The AC of OCT signal intensity reached its maximum (3.48 ± 0.37 mm⁻¹) in the top area and the minimum (2.68 ± 0.82 mm⁻¹) in the bottom area of the chose region in normal colon tissue. But for cancerous colon tissue, the corresponding values were 8.48 ± 0.95 mm⁻¹ and 3.16 ± 0.69 mm⁻¹, respectively. In both cases, the differences were significant ($p < 0.05$). In our experiments the AC of cancerous tissue was quite higher than that of normal tissue in Fig. 6. Cancerous tissue had a

higher concentration of hemoglobin, microvascular volume, blood content and protein that consisted mainly of red blood cells, hemachrome and fibrin, as compared with the surrounding unaffected tissue. These elements are known to have a high scattering property, which may explain that the higher AC values were seen in the cancerous tissue.⁴¹ The specificity and sensitivity were obtained based on the experimental data through comparing the average values of normal ($n = 11$) and malignant ($n = 11$) colon tissue groups. The specificity and sensitivity of PC was 81.8% and 72.7%, while specificity and sensitivity of AC was 81.8% and 63.6%, respectively. Although the specificity and sensitivity of PC and AC is helpful for the detection of normal and malignant colon tissues, combination of these values with excisional biopsy and histopathology is necessary to differentiate the tissues in practical applications.

This experiment presented the preliminary results of glucose permeability and optical attenuation in normal and cancer tissues *ex vivo* using SD-OCT technology. The differentiation between different types of colon tissue is based on alterations in the morphology of the tissues, such as the structural appearance, tissue characterization, and concentration of blood. Alterations in the organization of cells and tissue that composed the adenomas could influence the permeability of agents and optical attenuation in the tissue. The results showed that there was considerable variation in glucose permeability and optical attenuation between normal and malignant colon tissues. Therefore, SD-OCT technology could assist in the early detection and discrimination of tumors by monitoring and quantifying the diffusion of a hyperosmotic agent, as well as the difference of optical AC in the normal and cancerous tissues by SD-OCT imaging.

However, it should be noted that our experiments were performed *ex vivo* rather than *in vivo*. The optical properties of excised tissue could change from live tissue. In addition, we measured the samples at room temperature, which may also have a little influence on the results since the optical properties of tissue are temperature-dependent.⁴⁴ Therefore, an *in vivo* investigation is needed to identify these differences on the measurement.

4 Conclusions

In this paper, we have measured the optical AC and PC of glucose from normal and malignant colon tissue groups using the SD-OCT, and analyzed the changes of optical AC and PC during the region of interest. The results of this study have shown that the malignant colon tissue has higher optical AC and PC than

that present in normal colon tissue. These findings also suggest that quantitative analysis of colon tissue optical properties by the SD-OCT technology could benefit the differentiation of the adenomatous human colon tissue from normal tissue and early diagnosis of gastrointestinal cancerous tissue.

Acknowledgments

The research is supported in part by the following grant: National Basic Research Program of China (Nos. 2011CB707504 and 2010CB933903), National Natural Science Foundation of China (81171377, 61273368). The authors thank Dr. T. FitzGibbon for comments and suggestions on earlier drafts of the manuscript.

References

1. http://en.wikipedia.org/wiki/Colorectal_cancer.
2. S. A. Skinner, G. M. Frydman, and P. E. O'Brien, "Microvascular structure of benign and malignant tumors of the colon in humans," *Digest* **40**(2), 373–384 (1995).
3. Y. Furuya and T. Ogata, "Scanning electron microscopic study of the collagen networks of the normal mucosa, hyperplastic polyp, tubular adenoma and adenocarcinoma of the human large intestine," *J. Exp. Med.* **169**(1), 1–19 (1993).
4. J. F. Toussaint et al., "Water diffusion properties of human atherosclerosis and thrombosis measured by pulse field gradient nuclear magnetic resonance," *Arterioscler. Thromb. Vasc. Biol.* **17**(3), 542–546 (1997).
5. L. P. Hariri et al., "Endoscopic optical coherence tomography and laser-in a murine colon cancer model," *Lasers Surg. Med.* **38**(4), 305–313 (2006).
6. A. Das et al., "High-resolution endoscopic imaging of the GI tract: a comparative study of optical coherence tomography versus high frequency catheter probe," *Gastrointest. Endosc.* **54**(2), 219–224 (2001).
7. S. Yuan et al., "Simultaneous morphology and molecular imaging of colon cancer," in *IEEE/NIH Life Science Systems and Applications Workshop*, Vol. 978, pp. 167–169, IEEE, Bethesda, MD (2009).
8. K. V. Larin et al., "Quantification of glucose diffusion in arterial tissues by using optical coherence tomography," *Laser Phys. Lett.* **4**(4), 312–317 (2007).
9. H. Xiong et al., "Application of hyperosmotic agent to determine gastric cancer with optical coherence tomography ex vivo in mice," *J. Biomed. Opt.* **14**(2), 024029 (2009).
10. H. Q. Zhong et al., "Quantification of glycerol diffusion in human normal and cancer breast tissues in vitro with optical coherence tomography," *Laser Phys. Lett.* **7**(4), 315–320 (2010).
11. M. G. Ghosn, V. V. Tuchin, and K. V. Larin, "Nondestructive quantification of analyte diffusion in cornea and sclera using optical coherence tomography," *Invest. Ophthalmol. Visual Sci.* **48**(6), 2726–2733 (2007).
12. X. Guo et al., "In vivo quantification of propylene glycol, glucose and glycerol diffusion in human skin with optical coherence tomography," *Laser Phys.* **20**(9), 1849–1855 (2010).
13. D. J. Faber et al., "Quantitative measurement of attenuation coefficients of weakly scattering media using optical coherence tomography," *Opt. Express* **12**(19), 4353–4365 (2004).
14. C. Xu et al., "Characterization of atherosclerosis plaques by measuring both backscattering and attenuation coefficients in optical coherence tomography," *J. Biomed. Opt.* **13**(3), 034003 (2008).
15. V. M. Kodach et al., "Determination of the scattering anisotropy with optical coherence tomography," *Opt. Express* **19**(7), 6131–6140 (2011).
16. H. Q. Zhong et al., "In vitro study of ultrasound and different-concentration glycerol-induced changes in human skin optical attenuation assessed with optical coherence tomography," *J. Biomed. Opt.* **15**(3), 036012 (2010).
17. F. J. van der Meer et al., "Apoptosis- and necrosis-induced changes in light attenuation measured by optical coherence tomography," *Lasers Med. Sci.* **25**(2), 259–267 (2010).
18. K. V. Larin et al., "Noninvasive blood glucose monitoring with optical-coherence tomography: a pilot study in human subjects," *Diabetes Care* **25**(12), 2263–2267 (2002).
19. P. Karande and S. Mitragotri, "Dependence of skin permeability on contact area," *Pharm. Res.* **20**(2), 257–263 (2003).
20. Y. Liu et al., "Ultrasound-enhanced drug transport and distribution in the brain," *AAPS. Pharm. Sci. Tech.* **11**(3), 1005–1017 (2010).
21. Q. L. Zhao et al., "Depth-resolved monitoring of diffusion of hyperosmotic agents in normal and malignant human esophagus tissues using optical coherence tomography in-vitro," *Quantum Electron.* **41**(10), 950–955 (2011).
22. A. N. Bashkatov et al., "Monte Carlo study of skin optical clearing to enhance light penetration in the tissue: implications for photodynamic therapy of acne vulgaris," *Proc. SPIE* **7022**, 702209 (2008).
23. F. P. Bolin et al., "Refractive index of some mammalian tissues using a fiber optic cladding method," *Appl. Opt.* **28**(12), 2297–2303 (1989).
24. V. V. Tuchin, "Optical clearing of tissues and blood using the immersion method," *J. Phys. D.* **38**(15), 2497–2518 (2005).
25. K. V. Larin et al., "Specificity of noninvasive blood glucose sensing using optical coherence tomography technique: a pilot study," *Phys. Med. Biol.* **48**(10), 1371–1390 (2003).
26. R. O. Esenaliev et al., "Noninvasive monitoring of glucose concentration with optical coherence tomography," *Opt. Lett.* **26**(13), 992–994 (2001).
27. M. G. Ghosn et al., "Differential permeability rate and percent clearing of glucose in different regions in rabbit sclera," *J. Biomed. Opt.* **13**(2), 021110 (2008).
28. A. T. Yeh and J. Hirshburg, "Molecular interactions of exogenous chemical agents with collagen-implications for tissue optical clearing," *J. Biomed. Opt.* **11**(1), 014003 (2006).
29. M. G. Ghosn et al., "Monitoring of glucose permeability in monkey skin in vivo using Optical Coherence Tomography," *J. Biophoton.* **3**(1), 25–33 (2010).
30. Q. L. Zhao et al., "Quantifying glucose permeability and enhanced light penetration in ex vivo human normal and cancerous esophagus tissues with optical coherence tomography," *Laser Phys. Lett.* **8**(1), 71–77 (2011).
31. M. G. Ghosn, V. V. Tuchin, and K. V. Larin, "Depth-resolved monitoring of glucose diffusion in tissues by using optical coherence tomography," *Opt. Lett.* **31**(15), 2314–2316 (2006).
32. A. I. Kholodnykh et al., "Precision of measurement of tissue optical properties with optical coherence tomography," *Appl. Opt.* **42**(16), 3027–3037 (2003).
33. D. Levitz et al., "Determination of optical scattering properties of highly-scattering media in optical coherence tomography images," *Opt. Express* **12**(2), 249–259 (2004).
34. Y. Yang et al., "Optical scattering coefficient estimated by optical coherence tomography correlates with collagen content in ovarian tissue," *J. Biomed. Opt.* **16**(9), 090504 (2011).
35. L. Thrane, H. T. Yura, and P. E. Andersen, "Analysis of optical coherence tomography systems based on the extended Huygens-Fresnel principle," *J. Opt. Soc. Am. A* **17**(4), 484–490 (2000).
36. V. V. Tuchin, *Handbook of Coherent-domain Optical Methods: Biomedical Diagnosis, Environmental Monitoring*, 2nd ed., In Press, Springer-Verlag, New York (2012).
37. S. A. Boppert et al., "Optical coherence tomography: feasibility for basic research and image-guided surgery of breast cancer," *Breast Cancer Res. Treat.* **84**(2), 85–97 (2004).
38. R. K. Wang and V. V. Tuchin, "Enhance light penetration in tissue for high resolution optical imaging techniques by use of biocompatible chemical agents," *J. X-Ray Science Tech.* **10**(3), 167–176 (2002).
39. V. V. Tuchin et al., "Light propagation in tissues with controlled optical properties," *J. Biomed. Opt.* **2**(4), 401–417 (1997).
40. M. Wojtkowski et al., "Three-dimensional retinal imaging with high speed ultrahigh resolution optical coherence tomography," *Ophthalmol.* **112**(10), 1734–1746 (2005).
41. F. J. van der Meer et al., "Localized measurement of optical attenuation coefficients of atherosclerotic plaque constituents by quantitative optical coherence tomography," *IEEE Trans. Med. Imag.* **24**(10), 1369–1376 (2005).
42. T. G. Van Leeuwen, D. J. Faber, and M. C. Aalders, "Measurement of the axial point spread function in scattering media using single-mode fiber-based optical coherence tomography," *IEEE J. Sel. Topics Quantum Electron.* **9**(2), 227–233 (2003).
43. V. V. Tuchin, "Coherent optical techniques for the analysis of tissue structure and dynamics," *J. Biomed. Opt.* **4**(1), 100–125 (1999).
44. J. W. Pickering et al., "Changes in the optical properties (at 632.8 nm) of slowly heated myocardium," *Appl. Opt.* **32**(4), 367–371 (1993).